

Molecular Palladium Precursors for Pd⁰ Nanoparticle Preparation by Microwave Irradiation: Synthesis, Structural Characterization and Catalytic Activity

Frank Heinrich,^[a] Michael T. Keßler,^[a] Stephan Dohmen,^[a] Mrityunjay Singh,^[b] Martin H. G. Precht,^{*[a]} and Sanjay Mathur^{*[a]}

Keywords: Palladium / Complexes / Nanoparticles / Cross-coupling / Heck reaction / Wood

Two new palladium complexes [Pd(MEA)₂Cl₂] (**1**) and [Pd(MEA)₂Br₂] (**2**) [MEA = (2-methoxyethyl)amine] were synthesized by the reaction of 2 equiv. of MEA with PdCl₂ or [(cod)PdBr₂] (cod = cycloocta-1,5-diene), respectively. Single-crystal X-ray diffraction analysis of **1** and **2** revealed the formation of square-planar *trans* complexes with palladium coordinated by chloride/bromide ions and N-atoms of MEA bonded in a monodentate fashion. Given their molecular form and solubility, **1** and **2** act as intractable precursors to Pd nanoparticles by microwave-assisted synthesis. The influence of the reaction temperature, irradiation time and surfactant (PVP) concentration on the size (5–40 nm) of the re-

sulting particles was studied by DLS (hydrodynamic diameter) and TEM analyses (particle size). The growth mechanism of the nanoparticles depended on the type of halide ligand. Powder X-ray diffractometry confirmed the formation of elemental Pd particles that were embedded in carbonized wood to examine their potential as a catalyst. The catalytic activity of these nanoscale particles was evaluated in carbon-carbon cross-coupling reactions by using Heck, Suzuki and Sonogashira reactions as benchmark models. The investigations included recycling experiments that resulted in total turnover numbers of 4321 (Heck), 6173 (Sonogashira) and 8223 (Suzuki).

Introduction

Palladium in the form of molecular complexes, nanoparticles and films is of significant interest due to its high catalytic activity and application in organic synthesis; for example, hydrogenation reactions or organic cross-coupling reactions (e.g. Heck, Stille, Suzuki and Sonogashira) are well known and widely described in the literature. Palladium-based systems, which have been mostly obtained with ligands such as phosphanes, have been demonstrated as active reagents for homogeneous or heterogeneous catalysis with high turnover numbers (TONs). Generally, the observed TONs are lower for heterogeneous catalysts. However, they are of potential interest due to the ease of purification of the resulting products and superior recycling efficiency when compared to the corresponding homogeneous systems. Nevertheless, a comparative evaluation between homogeneous and heterogeneous catalytic systems is not straightforward and is subject to a variety of physicochemical parameters.^[1]

Furthermore, palladium anchored on metal oxide (MO_x) substrates serve as excellent catalysts for the decomposition of volatile organic components (VOCs) and other environmental pollutants (NO_x, CO). In addition, Pd/MO_x heterostructures are well suited for the detection of toxic gases (CO, CH₄).^[2] The extraordinary uptake of hydrogen in Pd structures has also led to new applications in the field of hydrogen storage and detection.^[3]

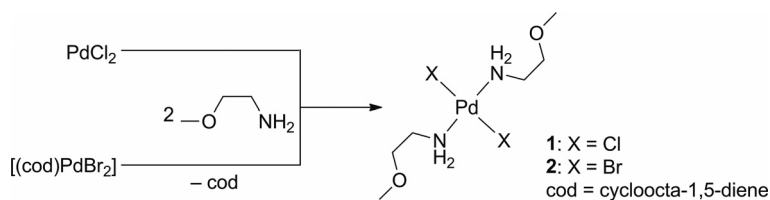
Palladium nanoparticles (Pd NPs) are of current interest due to their large surface/volume ratio and the possible control over their size and shape, which influences their catalytic properties.^[4,5] So far, many methods have been reported to prepare monodispersed Pd nanoparticles, which include chemical reduction of palladium salts or complexes^[6] by reaction with molecular hydrogen, metal hydrides or by means of the polyol process,^[5] or sonochemical methods^[7] whereby different surfactants, polymers or ionic liquids have been used to prevent agglomeration and to impose a chemical control over the morphological features of the particles.^[8]

Microwave irradiation of ionic or thermally labile precursors offers a facile, fast and green pathway to synthesize metal and metal oxide nanoparticles as the reaction durations are drastically reduced due to instantaneous heating of the reaction medium and formation of hot spots in the reaction mixture, which can be tuned by choosing solvents with desired polarity and dielectric properties.^[9] To this end, a number of ionic precursors, such as PdCl₄²⁻, PdCl₂

[a] Department of Chemistry, Chair of Inorganic and Materials Chemistry, University of Cologne, 50939 Cologne, Germany
E-mail: sanjay.mathur@uni-koeln.de
Homepage: www.mathur.uni-koeln.de

[b] NASA Glenn Research Center, Ohio Aerospace Institute, Cleveland, OH 44135-3191, USA

Supporting information for this article is available on the WWW under <http://dx.doi.org/10.1002/ejic.201200380>

Scheme 1. Syntheses of the palladium complexes **1** and **2**.

and Pd(OAc)₂ as well as neutral complexes like Pd₂(dba)₃ (dba = dibenzylideneacetone), have been successfully used in the microwave-assisted synthesis of Pd nanoparticles.^[10] The presence of a polar Pd complex in a polar solvent facilitates the interaction with the microwave field and results in a rapid heating and subsequent burst of decomposition reactions. The fast energy transfer and instantaneous decomposition of precursor species result in a brief nucleation stage producing well-dispersed particles with uniform size distribution.

We report here two new Pd complexes that exhibit lower decomposition temperatures and higher solubilities in common organic solvents compared to some other Pd precursors. Their ability to form palladium nanoparticles in the presence of PVP and ethanol by means of microwave-assisted decomposition has been tested and the influence of different reaction parameters and precursor configurations (Pd–Cl and Pd–Br units) on the size and shape of the particles was investigated. The Pd NPs were then embedded in carbonized wood and evaluated as recyclable precatalysts in ligand-free carbon–carbon cross-coupling reactions, namely the Heck, Suzuki and Sonogashira reactions.

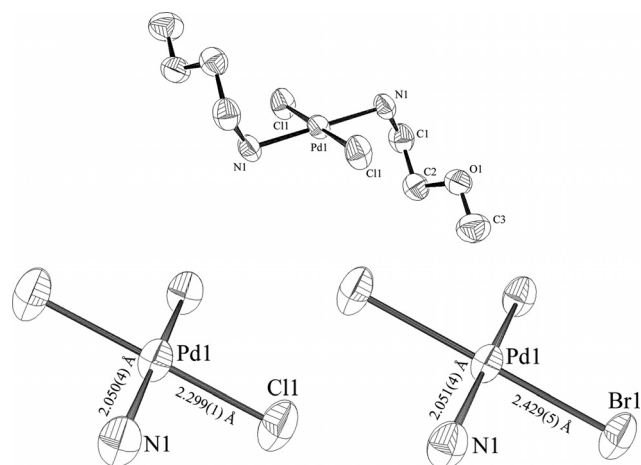
Results and Discussion

Reaction of PdCl₂ or [(cod)PdBr₂] (with cod = cycloocta-1,5-diene) with 2 equiv. of (2-methoxyethyl)amine resulted in the formation of complexes **1** and **2** as orange and yellowish compounds, respectively (Scheme 1). The products were characterized as discrete molecular species by single-crystal X-ray diffractometry, ¹H NMR spectroscopy, mass spectrometry, CHNS analysis and DSC/TGA analysis.

Single-Crystal X-ray Crystallography

The molecular structures of **1** and **2** are isotypical (Figure 1). Both compounds crystallize in the monoclinic space group *P*2₁/*c* where the unit cell of the dibromo derivative has a slightly higher cell volume (ca. 5.6%) due to the bulkier Br atoms.

In addition to the halide atoms, two monodentate (2-methoxyethyl)amine molecules are coordinated to the Pd centre to complete the observed square-planar coordination around the central metal atom. The Pd–N distances are around 2.05 Å for both of the compounds, the Pd–Cl distance (**1**) was found to be 2.30 Å, while the Pd–Br distance

Figure 1. Molecular structure of **1** and coordination spheres of **1** and **2**. Ellipsoids are drawn with 50% probability level, hydrogen atoms are not depicted for clarity.

(**2**) was 2.43 Å. The N–Pd–X [X = Cl (**1**), Br (**2**)] angles (89.18–90.82°) are very close to the optimal angle of 90°. Selected crystallographic data are given in Table 1.

Table 1. Selected crystallographic data for **1** and **2**.

	1	2
Empirical formula	C ₆ H ₁₈ Cl ₂ N ₂ O ₂ Pd	C ₆ H ₁₈ Br ₂ N ₂ O ₂ Pd
Formula mass [g mol ⁻¹]	327.52	416.44
Crystal system	monoclinic	monoclinic
Space group	<i>P</i> 2 ₁ / <i>c</i>	<i>P</i> 2 ₁ / <i>c</i>
<i>a</i> [Å]	8.566(2)	8.503(1)
<i>b</i> [Å]	8.605(1)	8.936(1)
<i>c</i> [Å]	8.987(2)	9.226(2)
β [°]	113.08(2)	113.34(2)
<i>Z</i> / <i>V</i> [Å ³]	2/609.4(2)	2/643.6(2)
θ range [°]	2.58–29.61	3.31–28.08
<i>T</i> [K]	293(2)	293(2)
Index range	–11 < <i>h</i> < 11 –11 < <i>k</i> < 11 –12 < <i>l</i> < 12	–11 < <i>h</i> < 11 –11 < <i>k</i> < 11 –12 < <i>l</i> < 12
Total data collected	8395	6008
Unique data	1699	1555
Observed data	1070	1114
<i>R</i> _{merg}	0.0423	0.0539
μ [mm ⁻¹]	1.936	7.627
<i>R</i> indexes [<i>I</i> > 2 σ (<i>I</i>)]	<i>R</i> ₁ = 0.0427 <i>wR</i> ₂ = 0.1012	<i>R</i> ₁ = 0.0349 <i>wR</i> ₂ = 0.0792
<i>R</i> indexes (all data)	<i>R</i> ₁ = 0.0719 <i>wR</i> ₂ = 0.1177	<i>R</i> ₁ = 0.0559 <i>wR</i> ₂ = 0.0841
Goof	0.992	1.031

Thermal Properties

The thermal behaviour of **1** and **2** was analyzed by thermogravimetry and differential scanning calorimetry (TGA/DSC) measurements under air (Figure 2). Both **1** and **2** showed an endothermic feature without any significant weight loss up to 110 °C, which was attributed to the melting of the compounds, while at 200 °C the onset of decomposition was observed, which resulted in elemental palladium. The observed weight losses were very close to the theoretical values of 33% (calcd. 33%) for compound **1** and 27% (calcd. 26%) for compound **2**. No further weight reduction after 550 °C confirmed the formation of stable final products.

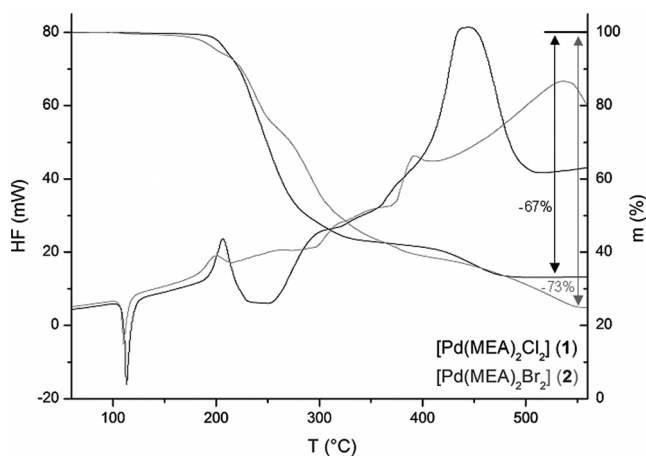


Figure 2. DSC/TGA plots for **1** and **2**.

Microwave-Assisted Synthesis of Pd Nanoparticles

Compounds **1** and **2** were used as precursors in the microwave-assisted synthesis of Pd nanoparticles as they show low decomposition temperatures and good solubilities in common organic solvents. Exposure of the ethanolic solutions of **1** and **2** to microwave treatment induced the reduction reaction that led to elemental Pd. A remarkable colour change from yellow to dark brown during the microwave irradiation indicated the reduction of Pd^{II} to Pd⁰, which sedimented in the form of a black powder; however, stable dispersions could be obtained by the addition of polyvinylpyrrolidone (PVP 40000), which acted as an efficient capping agent for the nanocrystals. As shown in the powder XRD pattern (Figure 3), elemental Pd in *fcc* phase was formed. The peaks at 40°, 47° and 68° correspond to the {111}, {200} and {220} lattice planes (JCPDS card no. 00-046-1043). According to the Scherrer equation a crystallite size of 8.7 nm (±0.9 nm) was obtained.

The concentration of PVP, the reaction temperature and the time of microwave irradiation during the decomposition process were changed, and the influence of these changes on the particle size (hydrodynamic diameter) was analyzed by dynamic light scattering (DLS) measurements.

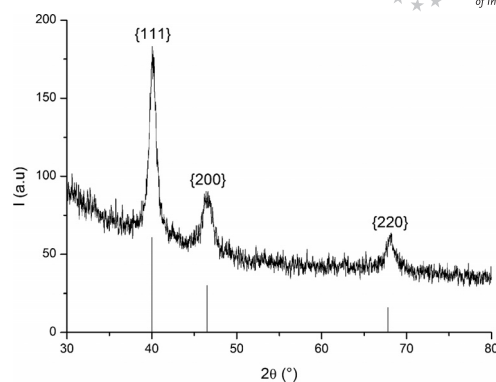


Figure 3. Powder XRD pattern of the as-synthesized Pd nanoparticles obtained from **1** with 20 mg of PVP, microwave irradiation time 5 min and temperature 150 °C.

Despite their isotypical crystal structures and similar decomposition profiles (TGA/DSC data), the microwave-assisted reduction of **1** and **2** led to palladium nanoparticles of different sizes. Apparently, the palladium–halogen bond becomes stronger in going from chloride to bromide, which results in a faster reduction of **1** under similar experimental conditions. Consequently, the faster growth of Pd nuclei leads to a faster formation of nanocrystals, as observed in the DLS measurements. In most of the reactions the particles are larger when complex **2** was used. The formation of Pd particles by microwave irradiation occurs at 130 °C for compound **1** and at 150 °C for compound **2** when applying a power of 150 W.

By enhancing the PVP/precursor ratio, the hydrodynamic diameter decreases in the case of compound **1** from about 48 nm (10 mg of PVP) to 37 nm (30 mg of PVP). In the case of compound **2**, these changes lead to an enhancement of the hydrodynamic diameter (from 47 to 54 nm) (Figure 4).

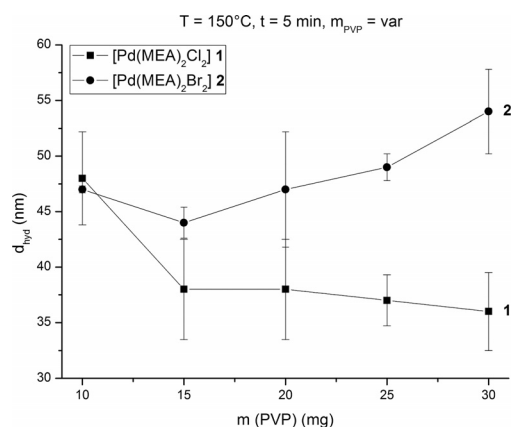


Figure 4. Mass of PVP vs. hydrodynamic diameter for Pd particles synthesized by using **1** and **2** with microwave irradiation time of 5 min and temperature of 150 °C.

The effect of the microwave irradiation time on the particle size did not exhibit a linear relationship. For compound **1**, after 3 and 4 min irradiation time the hydrodynamic diameters were in the range of 30–32 nm. After

5 min, the diameter increased to 37 nm and decreased to 33 nm at an irradiation time of 7 min. In the case of compound **2**, the hydrodynamic diameters increased from 42 to 63 nm on increasing the irradiation time from 3 min to 7 min, respectively, as shown in Figure 5.

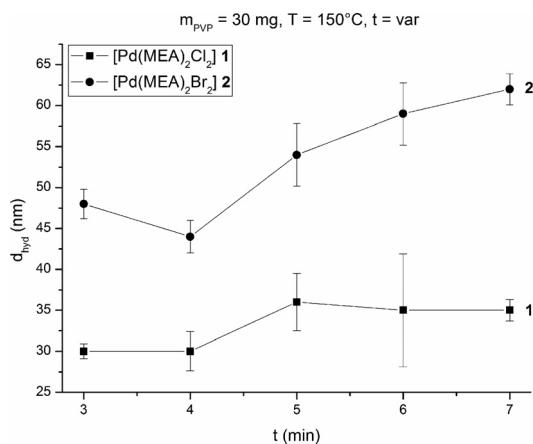


Figure 5. Irradiation time vs. hydrodynamic diameter for Pd particles synthesized by using **1** and **2** with a temperature of 150 °C and 30 mg PVP.

Evidently, the synthesis temperature critically influences the size of the formed particles when the chloride-containing compound is used. At higher temperatures larger particles are formed (130 °C: 34 nm; 170 °C: 68 nm). At 110 °C no particles were obtained. Again the bromide-containing compound shows a different behavior. At temperatures lower than 150 °C no particles precipitated upon centrifugation. At 150 °C and 170 °C the hydrodynamic diameters of the particles are around 50 nm.

It is well known that the growth mechanism of Pd particles is directly influenced by the halide ions present in the solution and, as reported by Xia et al.,^[4,5] the addition of halide ions can change or rebuild the morphology of the as-formed nanoparticles. They observed that the adsorption of Br⁻ ions on the surface of growing Pd nanoparticles promotes the formation of {100} facets. In their studies mainly nanocubes and nanobars of Pd were obtained, whereas upon using chloride-containing compounds and/or surfactants mainly polyhedral structures were observed. The shape of the resulting nanoparticles depends on the etching power of the halide ions; in the case of Ag NPs, which also crystallizes in the *fcc* phase, the presence of Cl⁻ ions produced Ag nanocubes, while the milder etchant Br⁻ enables the formation of bipyramidal particles.^[5]

In addition, ions that are charged oppositely to the surface charge of NPs can strongly attenuate the influence of electrostatic double layer repulsion by neutralizing the surface charge on the NPs, which can further affect the growth kinetics. Dyson et al. in the course of the nanoparticle synthesis that used palladium halides in imidazolium ionic liquids isolated stable palladium–carbene complexes with halide ligands in addition to palladium nanoparticles.^[11c] This shows the influence of in situ complexation

of ligands and their influence on the kinetics of the reduction, which affects the particle growth.

The electron microscopy analysis revealed that the particles obtained from compound **1** at 130 °C showed a high degree of polydispersity. This temperature is too low to ensure spontaneous nucleation, and therefore the resulting particles show variable diameters and size-dispersion. The particles obtained from **2** are less monodisperse than those obtained from compound **1**. The particles do not have unique shapes but are elongated. The diameters of the nanoparticles were between 5 and 40 nm, whereas the aspect ratio of the elongated structure was < 10. TEM images confirmed the crystallinity of the particles in all of the measured samples (Figure 6).

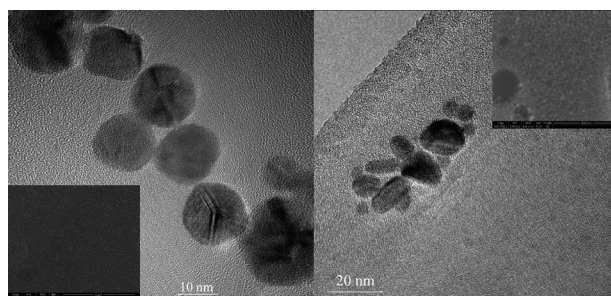


Figure 6. TEM and SEM images of Pd NPs derived from **1** (left) and **2** (right). Mass of PVP 30 mg, temperature 150 °C, power 150 W, irradiation time 5 min in both cases.

Catalytic Activity

Palladium is known for its high catalytic activity in carbon–carbon cross-coupling reactions.^[1,11] Traditionally, those reactions were carried out with defined palladium complexes or with palladium salts in the presence of phosphane, carbene or amine ligands.^[11] In the last two decades it has been proven that ligand-free approaches involving molecular species and nanoparticles dissolved in a monophasic or biphasic reaction mixture play an important role in the catalytic cycle.^[11] It should be pointed out that the nanoparticles act as a reservoir for molecular species.^[1c,11,12] The advantage of nanoparticle-based systems is their long-term stability compared to that of metal complexes. However, to make this property of nanoparticles useful in recyclable catalyst systems, the Pd NPs should be well immobilized in a liquid support or grafted onto a solid support.^[1c] In this manner the product phase can simply be separated from the catalyst by decantation or filtration. In the present work we embedded in situ synthesized palladium nanoparticles into carbonized cherry wood, which shows good structural features and means a very homogeneous distribution of channels. These channels could be filled with Pd NPs by decomposition of the dissolved palladium complexes **1** and **2** under microwave irradiation in the presence of pieces of wood. SEM measurements revealed that the wood was uniformly decorated with Pd nanoparticles (Figure 7).

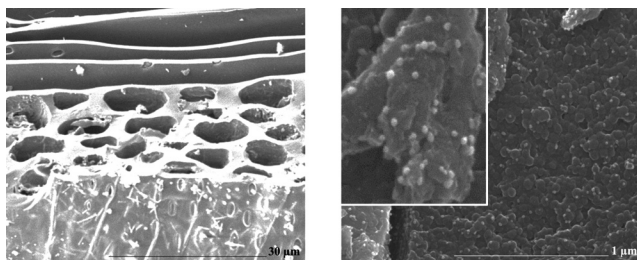
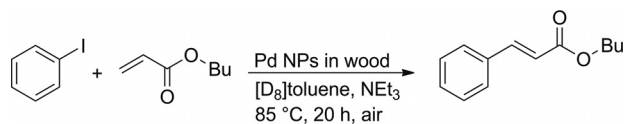


Figure 7. SEM images of empty wood channels (left) and wood channels decorated by Pd nanoparticles (right).

After impregnation of the wood with the PVP-protected palladium nanoparticles, the resulting material was evaluated in established carbon–carbon cross-coupling reactions to estimate their catalytic activity. The Heck reaction is well known to be promoted by Pd NPs as the catalyst reservoir.^[1c,11,12] Therefore, we decided to couple iodobenzene with *n*-butyl acrylate in the presence of triethylamine and PVP-Pd@wood (1.35 μmol Pd content; 0.14 wt.-% Pd) at 85 °C yielding butyl cinnamate in 57% (TON: 1407) in the first run (Scheme 2; Figure 8). The magic-number methodology was used for the calculation of the TONs based on the surface atoms of the metal nanoparticles.^[13] A spherical crystallite of 8.7 nm (± 0.9 nm) contains roughly 23485 atoms within 20 shells. The surface shell contains 3500 atoms, and hence 15% of the atoms are surface atoms, which may potentially act as a catalyst reservoir. Figure 8 depicts the TONs of the recycling experiments in five runs taking only the surface atoms into account. The graphical sketch of the TONs may lead to the idea that strong catalyst leaching occurs during the consecutive recycling experiments. However, ICP-MS analysis of the catalyst material before and after the catalysis revealed that the palladium content does not change drastically, as will be discussed later (Suzuki reaction). After each run the catalyst material was separated from the formed ammonium salt and the product phase. In the following recycling experiments the conversions decreased down to 494 TONs or 20% (Figure 8). Nevertheless, the very low Pd-loading gives remarkably high TONs in all of the runs (Figure 8) and a total TON for all runs of 4321.



Scheme 2. Heck coupling reaction performed to test the efficacy of new heterogeneous catalysts.

In further experiments we optimized the reaction conditions for C–C coupling reactions and performed the copper-free Sonogashira coupling of phenyl iodide and phenylacetylene in ethanol with potassium carbonate at 50 °C within 1 d (Scheme 3; Figure 9). In this case, the TON reached 3704 (75% conversion) in the initial run, the TONs dropped in every recycle and then stabilized in the third and fourth run to between 440 and 500.

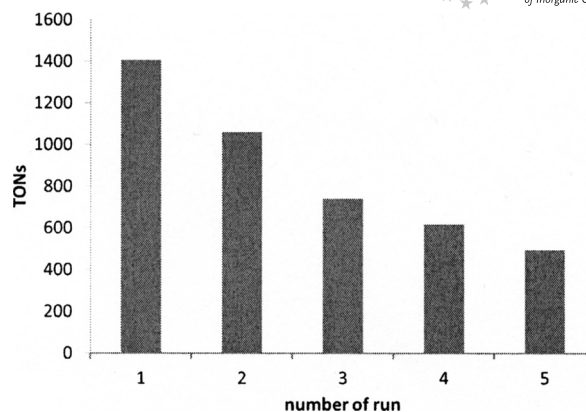
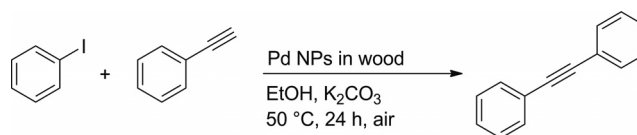


Figure 8. Recycling experiments in the Heck reaction.



Scheme 3. Sonogashira coupling reaction.

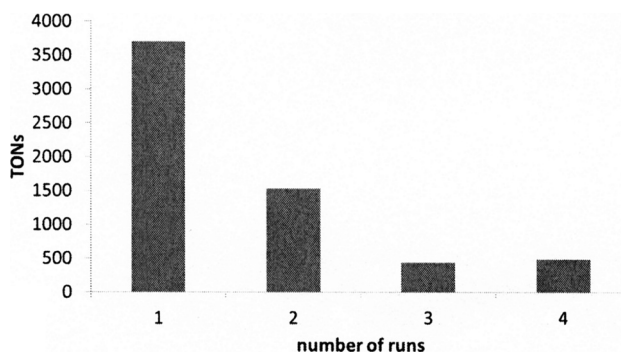
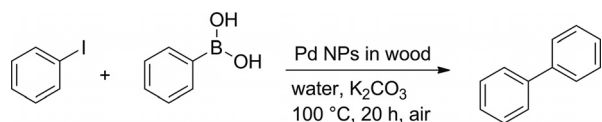


Figure 9. Recycling experiments in the Sonogashira reaction.

Furthermore, Suzuki reactions were performed with the PVP-Pd@wood catalyst in water as reaction media at 100 °C for 20 h (Scheme 4; Figure 10). The product is formed in the first two runs in high conversions (84–97%; 2074 and 2395 TONs) and can easily be isolated by extraction with pentane. The catalyst recycling shows remarkably high conversions in the first two runs in this biaryl coupling, and then the TONs decrease. The total TON over six runs reached 8223. ICP-MS analysis of the catalyst material before and after the catalysis reaction revealed that the palladium content does not change drastically. The prepared catalyst embedded onto wood contained 1.35 μmol palladium, and after the catalysis the palladium content was found to be 1.30 μmol. This indicates that the activity did not drop due to extensive metal leaching and that the deactivation must be related to another parameter. Considering the catalyst support, we assume that significant amounts of triethylammonium iodide that formed as byproduct may clog the pores and channels of the support material after each run. Consequently, fewer nanoparticles were available to act as the catalyst reservoir.



Scheme 4. Suzuki coupling reaction in water.

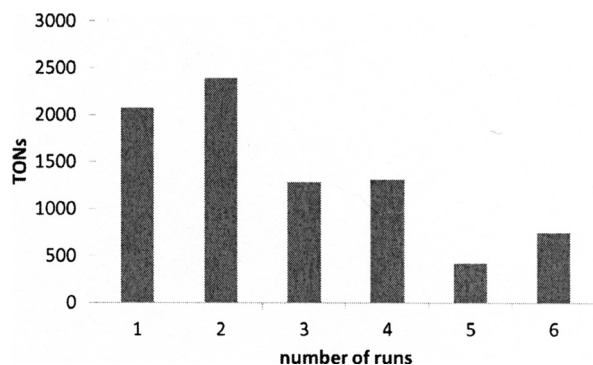


Figure 10. Recycling experiments in the Suzuki reaction in water.

Conclusions

Two new palladium complexes were synthesized, characterized and used as precursors for the formation of Pd nanoparticles by means of microwave irradiation. DLS and SEM/TEM measurements show that the resulting shape and size of the crystalline particles is influenced by the halide content in the compounds. The particles were embedded into carbonized wood, and their catalytic activity was confirmed by Heck, copper-free Sonogashira and Suzuki reactions in recycling experiments. The total TONs reached under optimized conditions were 4321 (Heck), 6173 (Sonogashira) and 8223 (Suzuki). The deactivation of the catalyst material is probably related to salts that clog the pores and channels of the wooden matrices as no metal leaching was observed.

Experimental Section

General: [(cod)PdBr₂] was synthesized from K₂PdBr₄,^[14] which was obtained from elemental palladium^[15] according to literature procedures. The wooden templates were prepared by carbonization of wood (cherry wood) at 1000 °C in vacuo. All of the other chemicals were applied without further purification. ¹H NMR spectra were recorded with a Bruker AVANCE II 300 spectrometer at 298 K (300.1 MHz, external standard TMS). C, H and N analyses were carried out with a HEKATEch Euro EA 3000 apparatus. Positive EI mass spectra were recorded with a Finnigan MAT 95 apparatus. Thermogravimetric measurements were performed with a STARE System by Mettler Toledo with TGA/DSC1 and Gas Controller GC100. For the synthesis of the Pd NPs a microwave CEM Discover and a centrifuge Eppendorf Centrifuge 5702 were used.

X-ray Crystallographic Analysis of Precursors: Single-crystal analysis was carried out with a STOE IPDS I and II with Mo-*K*_α irradiation. The structure was solved with SHELXS and SIR-92, the refinement was done with SHELXL and WinGX. For absorption correction STOE X-RED and STOE X-SHAPE were used. The structures were drawn with Ortep-III. CCDC-847018 (for **2**) and

-847019 (for **1**) contain the supplementary crystallographic data for this paper. These data can be obtained free of charge from The Cambridge Crystallographic Data Centre via www.ccdc.cam.ac.uk/data_request/cif.

Characterization of Nanoparticles: The obtained Pd NPs were analyzed by powder X-ray diffractometry (STOE-STADI MP, Cu-*K*_α irradiation, λ = 1.540598 Å), SEM (Nano SEM 430 by FEI), EDX (Apollo X by EDAX), TEM (Philips CM300 FEG/UT-STEM) and DLS (Zetasizer Nano-ZS by Malvern). The ICP-MS measurements were carried out by IWA, Institut für Wasser- und Abwasseranalytik GmbH, 52070 Aachen.

[Pd(MEA)₂Cl₂] (1): PdCl₂ (100 mg, 0.564 mmol) was suspended in thf (20 mL). (2-Methoxyethyl)amine (103 μL, 89 mg, 1.184 mmol) was added and the mixture stirred for 12 h. The solvent was evaporated, and the resulting orange solid was washed with *n*-pentane (3 × 10 mL) and recrystallized from thf. The yield was 163 mg (88%). ¹H NMR (300 MHz, room temp., CDCl₃): δ = 3.54 (t, 2 H, CH₂O), 3.35 (s, 3 H, CH₃), 2.91 (m, 4 H, CH₂N, NH₂) ppm. ¹³C NMR (75 MHz, room temp., CDCl₃): δ = 71.1 (CH₂O), 58.8 (CH₃), 44.8 (CH₂N) ppm. C₆H₁₈Cl₂N₂O₂Pd (327.55): calcd. C 22.00, H 5.54, N 8.55; found C 21.23, H 5.78, N 8.01. MS (EI⁺, 20 eV, 140 °C): *m/z* (%) = 328 (2) [M]⁺, 292 (5) [M - HCl]⁺, 254 (8) [M - 2 HCl]⁺, 181 (3) [Pd(MEA)]⁺, 76 (4) [MEA + H]⁺, 75 (3) [MEA]⁺, 45 (28) [C₂H₅O]⁺, 44 (6) [C₂H₆N]⁺, 30 (100) [CH₄N]⁺.

[Pd(MEA)₂Br₂] (2): [(cod)PdBr₂] (200 mg, 0.534 mmol) was dissolved in thf (20 mL). (2-Methoxyethyl)amine (98 μL, 84 mg, 1.122 mmol) was added and the mixture stirred for 1 h. The solvent was evaporated, and the resulting orange-yellow solid was washed with *n*-pentane (3 × 10 mL) and recrystallized from thf. The yield was 195 mg (88%). ¹H NMR (300 MHz, room temp., CDCl₃): δ = 3.49 (t, 2 H, CH₂O), 3.35 (s, 3 H, CH₃), 2.97 (t, 2 H, CH₂N), 2.80 (br. s, 2 H, NH₂) ppm. ¹³C NMR (75 MHz, room temp., CDCl₃): δ = 71.1 (CH₂O), 58.8 (CH₃), 45.7 (CH₂N) ppm. C₆H₁₈Br₂N₂O₂Pd (416.45): calcd. C 17.30, H 4.36, N 6.73; found C 17.31, H 4.52, N 6.36. MS (EI⁺, 20 eV, 140 °C): *m/z* (%) = 337 (32) [M - Br]⁺, 255 (9) [M - 2 Br - H]⁺, 181 (3) [Pd(MEA)]⁺, 76 (3) [MEA + H]⁺, 75 (2) [MEA]⁺, 45 (26) [C₂H₅O]⁺, 44 (6) [C₂H₆N]⁺, 30 (100) [CH₄N]⁺; [M]⁺ could not be observed.

Pd Nanoparticles: In a typical synthesis precursor **1** (20 mg, 0.061 mmol) or **2** (25 mg, 0.061 mmol) was mixed with PVP 40000 (10–30 mg) and dissolved in ethanol (4 mL) in a microwave tube. The microwave treatment took place while stirring the mixture at 130–170 °C for 3–7 min. The resulting dark brownish solution was centrifuged at 11 krpm for 30–60 min, the surfactant was removed, ethanol (10 mL) was added to the residue, and the mixture was centrifuged again using the same parameters. This washing process was repeated three times. The particles could easily be redispersed in ethanol to form stable dispersions. For the impregnation of wood, small pieces of wood were directly added to the reaction mixture prior to decomposition.

Heck Reaction with Pd NPs: In a typical experiment iodobenzene (55 μL, 0.5 mmol), *n*-butyl acrylate (72 μL, 0.5 mmol), triethylamine (80 μL, 0.6 mmol), PVP-Pd@wood (98 mg; 0.14 wt.-% Pd) and [D₈]toluene (1 mL) were introduced into a 20 mL reaction vial in air. The mixture was stirred at 85 °C for 20 h. Then the conversion was determined directly by ¹H NMR spectroscopy by using hexamethyldisilane as the internal standard (20 μL).

Sonogashira Reaction with Pd NPs: In a typical experiment phenyl acetylene (110 μL, 1.0 mmol), iodobenzene (120 μL, 1.1 mmol) and potassium carbonate (207 mg, 1.5 mmol) were added to ethanol (2 mL) and mixed with the PVP-Pd@wood (72 mg; 0.14 wt.-% Pd)

in a 20 mL reaction vial in air. The mixture was stirred at 50 °C for 24 h. The product was extracted with pentane (30 mL) from the reaction mixture, diluted with water (2 mL), the organic layer was dried with MgSO₄, and the solvent was removed under vacuum. The product was analyzed, and the conversion was determined by ¹H NMR spectroscopy by using hexamethyldisilane as the internal standard (20 μL).

Suzuki Reaction: In a typical experiment phenylboronic acid (91 mg, 0.75 mmol), iodobenzene (55 μL, 0.5 mmol), and potassium carbonate (140 mg, 1.0 mmol) were added to water (3 mL) and mixed with PVP-Pd@wood (72 mg; 0.14 wt.-% Pd) in a 20 mL reaction vial in air. The mixture was stirred at 100 °C for 20 h. At room temperature a crystalline solid precipitated from the water. The product was extracted with pentane (30 mL) from the aqueous phase, the organic layer was dried with MgSO₄, and the solvent was removed under vacuum. The white solid was analyzed, and the conversion was determined by ¹H NMR spectroscopy by using hexamethyldisilazane as the internal standard (20 μL).

Supporting Information (see footnote on the first page of this article): TEM images of the Pd nanoparticles are presented.

Acknowledgments

The authors gratefully acknowledge the University of Cologne and the Regional Research Cluster – Sustainable Chemical Systems (SusChemSys) for financial support. Thanks are due to Dr. H. Shen and J. Schläfer (TEM analysis), Dr. I. Pantenburg (single-crystal X-ray diffractometry), R. Fiz (SEM analysis), A. Baum (mass spectrometry), and S. Kremer (CHNS analysis) for their help and discussions. M. H. G. P. is thankful to the Ministry of Innovation, Science and Research of the state NRW (MIWF-NRW) for financial support.

- [1] a) C. Barnard, *Platinum Met. Rev.* **2008**, *52*, 38–45; b) X. F. Wu, P. Anbarasan, H. Neumann, M. Beller, *Angew. Chem.* **2010**, *122*, 9231; *Angew. Chem. Int. Ed.* **2010**, *49*, 9047–9050; c) M. H. G. Precht, J. D. Scholten, J. Dupont, *Molecules* **2010**, *15*, 3441–3461; d) R. Venkatesan, M. H. G. Precht, J. D. Scholten, R. P. Pezzi, G. Machado, J. Dupont, *J. Mater. Chem.* **2011**, *21*, 3030–3036; e) M. Lamblin, L. Nassar-Hardy, J.-C. Hierso, E. Fouquet, F.-X. Felpin, *Adv. Synth. Catal.* **2010**, *352*, 33–79.
- [2] a) Y. Liu, Z. Wu, Z. Sheng, H. Wang, N. Tang, J. Wang, *J. Hazard. Mater.* **2009**, *164*, 542–548; b) M. S. Hegde, G. Madras, K. C. Patil, *Acc. Chem. Res.* **2009**, *42*, 704–712; c) G. Centi, *J. Mol. Catal. A* **2001**, *173*, 287–312; d) V. G. Papadakis, C. A. Pliangos, I. V. Yentekakis, X. E. Verykios, C. G. Vayenas, *Catal. Today* **1996**, *29*, 71–75; e) M. V. Twigg, *Catal. Today* **2011**, *163*, 33–41; f) H. H. Choi, I. Kim, G.-H. Kim, S. D. Kim, *INEC: 2010 3rd International Nanoelectronics Conference* **2010**, *1–2*, 533–534; g) D.-J. Yang, I. Kamiyachick, D. Y. Youn, A. Rothschild, I.-D. Kim, *Adv. Funct. Mater.* **2010**, *20*, 4258–4264; h) J. Chen, K. Wang, R. Huang, T. Saito, Y. H. Ikuhara, T. Hirayama, W. Zhou, *IEEE T. Nanotechnol.* **2010**, *9*, 634–639.
- [3] a) J.-S. Noh, J. M. Lee, W. Lee, *Sensors* **2011**, *11*, 825–851; b) R. M. Penner, *MRS Bull.* **2010**, *35*, 771–777; c) E. Sennik, N. Kilinc, Z. Z. Ozturk, *J. Appl. Phys.* **2010**, *108*, 054317; d) S. R. Hunter, J. F. Patton, M. J. Sepaniak, P. G. Daskos, D. B. Smith, *Sensor Actuat. A: Phys.* **2010**, *163*, 464–470; e) V. A. Vons, H. Leegwater, W. J. Legerstee, S. W. H. Eijt, A. Schmidt-Ott, *Int. J. Hydrogen Energy* **2010**, *35*, 5479–5489.
- [4] a) Y. Xia, Y. Xiong, H. Cai, B. J. Wiley, J. Wang, M. J. Kim, *J. Am. Chem. Soc.* **2007**, *129*, 3665–3675; b) Y. Xia, Y. Xiong, H. Cai, Y. Yin, *Chem. Phys. Lett.* **2007**, *440*, 273–278; c) Y. Xia, Y. Xiong, J. M. McLellan, J. Chen, Y. Yin, Z.-Y. Li, *J. Am. Chem. Soc.* **2005**, *127*, 17118–17127.
- [5] a) Y. Xia, Y. Xiong, J. Chen, B. Wiley, *J. Am. Chem. Soc.* **2005**, *127*, 7332–7333; b) S. H. Im, Y. T. Lee, B. Wiley, Y. Xia, *Angew. Chem.* **2005**, *117*, 2192; *Angew. Chem. Int. Ed.* **2005**, *44*, 2154–2157.
- [6] a) H. Choo, B. He, K. Y. Liew, H. Liu, J. Li, *J. Mol. Catal. A* **2006**, *244*, 217–228; b) D. Li, S. Komarneni, *J. Nanosci. Nanotechnology* **2008**, *8*, 3930–3935.
- [7] Q. Shen, Q. Min, J. Shi, L. Jiang, J.-R. Zhang, W. Hou, J.-J. Zhu, *J. Phys. Chem. C* **2009**, *113*, 1267–1273.
- [8] a) P.-F. Ho, K.-M. Chi, *Nanotechnology* **2004**, *15*, 1059–1064; b) J. Dupont, J. D. Scholten, *Chem. Soc. Rev.* **2010**, *39*, 1780–1804.
- [9] a) S. Mathur, L. Xiao, H. Shen, R. von Hagen, J. Pan, L. Belkoura, *Chem. Commun.* **2010**, *46*, 6509–6511; b) M. N. Nadagouda, T. F. Speth, R. S. Varma, *Acc. Chem. Res.* **2011**, *44*, 469–478.
- [10] a) T. Huang, Y. Yu, Y. Zhao, H. Liu, *Mater. Res. Bull.* **2010**, *45*, 159–164; b) Y. X. Chen, B. L. He, H. F. Liu, *J. Mater. Sci. Technol.* **2005**, *21*, 187–190; c) L. H. Du, Y. G. Wang, *Synth. Commun.* **2007**, *37*, 217–222; d) A. da Conceicao Silva, J. D. Senra, L. C. S. Aguiar, A. B. C. Simas, A. L. F. de Souza, L. F. B. Malta, O. A. C. Antunes, *Tetrahedron Lett.* **2010**, *51*, 3883–3885; e) D. L. Martins, H. M. Alvarez, L. C. S. Aguiar, *Tetrahedron Lett.* **2010**, *51*, 6814–6817; f) Z. Du, W. Zhou, F. Wang, J. X. Wang, *Tetrahedron* **2011**, *67*, 4914–4918.
- [11] a) M. T. Reetz, E. Westermann, *Angew. Chem.* **2000**, *112*, 170; *Angew. Chem. Int. Ed.* **2000**, *39*, 165–168; b) S. W. Kim, M. Kim, W. Y. Lee, T. Hyeon, *J. Am. Chem. Soc.* **2002**, *124*, 7642–7643; c) A. Alimardanov, L. S. V. de Vondervoort, A. H. M. de Vries, J. G. de Vries, *Adv. Synth. Catal.* **2004**, *346*, 1812–1817; d) M. T. Reetz, J. G. de Vries, *Chem. Commun.* **2004**, 1559–1563; e) Z. F. Fei, D. B. Zhao, D. Pieraccini, W. H. Ang, T. J. Geldbach, R. Scopelliti, C. Chiappe, P. J. Dyson, *Organometallics* **2007**, *26*, 1588–1598.
- [12] a) C. C. Cassol, A. P. Umpierre, G. Machado, S. I. Wolke, J. Dupont, *J. Am. Chem. Soc.* **2005**, *127*, 3298–3299; b) C. S. Consorti, F. R. Flores, J. Dupont, *J. Am. Chem. Soc.* **2005**, *127*, 12054–12065; c) I. P. Beletskaya, A. N. Kashin, I. A. Khotina, A. R. Khokhlov, *Synlett* **2008**, *10*, 1547–1552; d) C. Rangheard, C. D. Fernandez, P. H. Phua, J. Hoorn, L. Lefort, J. G. de Vries, *Dalton Trans.* **2010**, *39*, 8464–8471.
- [13] A. P. Umpierre, E. de Jesus, J. Dupont, *ChemCatChem* **2011**, *3*, 1413–1418.
- [14] G. Brauer, *Handbuch der präparativen anorganischen Chemie*, Ferdinand Enke Verlag, Stuttgart, **1981**, vol. 3, p. 1377.
- [15] P. Heimbach, M. Molin, *J. Organomet. Chem.* **1973**, *49*, 483–494.

Received: April 17, 2012
 Published Online: October 19, 2012